block is attributable to hyperactivation of E2F1 and p53, suggesting that p57 deficiency disrupts the balance between p53 activity and pre-TCR signaling. Finally, we observed that additional ablation of p53 on the p57-null background resulted in the development of thymic lymphoma, indicating that the p57-p53 axis also functions as a suppressor of this fatal hematologic malignancy.

Methods

Generation of conditional knockout mice

Female mice heterozygous for a floxed *p57* allele ($p57^{[+]/F}$ or $p57^{[F]/+}$) were crossed with male Lck-Cre or CD4-Cre (kindly provided by C. B. Wilson, University of Washington, Seattle, WA) transgenic mice.[21-23] Deletion of *p57* in the resulting offspring was detected by polymerase chain reaction (PCR) analysis of genomic DNA with the primers AM83 (5′-ATGAGCGTCTG TTAGGGACAGAC-3′), AM84 (5′-GACCAGACAGTCGAAATGGTTC C-3′), and AM85 (5′-GCCGCGGTGTTGTTGAAACTG-3′). Lck-Cre/$p57^{[+]/+}$ or CD4-Cre/$p57^{[+]/+}$ mice were studied as controls for Lck-Cre/$p57^{[+]/F}$ or CD4-Cre/$p57^{[+]/F}$ mice, respectively. Lck-Cre/$p57^{[+]/F}$ mice were also crossed with $E2f1^{-/-}$ (kindly provided by L. Yamasaki, Columbia University, New York, NY) or $p53^{-/-}$ (Taconic, Hudson, NY) mice. The animal ethics committee of Kyushu University approved all mouse experiments.

Flow cytometry and cell sorting

Antibodies to mouse CD4 (RM4-5), CD8α (53-6.7), CD25 (3C7), CD44 (IM7), TCRβ (H57-597), B220 (RA3-6B2), TER119, Gr-1 (RB6-8C59), Mac-1 (M1/70), and NK1.1 (PK136) were obtained from BD Biosciences (San Jose, CA). CD4, CD8, B220, TER119, Gr-1, Mac-1, and NK1.1 were used as lineage markers. For determination of bromodeoxyuridine (BrdU) incorporation in vivo, mice were injected intraperitoneally with BrdU (1 mg) twice, with a 2-hour interval between injections. The thymus was harvested 1 hour after the second injection, and BrdU incorporation was evaluated with a BrdU Flow kit (BD Biosciences). For assay of apoptosis, thymocytes or splenic T cells were stained for cell surface markers, further incubated for 15 minutes with annexin V (BD Biosciences), and then analyzed by flow cytometry. For determination of intracellular TCRβ expression, cells were fixed in 2% paraformaldehyde after surface staining to determine thymocyte subsets, and they were then stained with antibodies to TCRβ in phosphate-buffered saline (PBS) containing 0.5% saponin and 4% fetal bovine serum. Stained cells were analyzed and sorted with the use of FACSCalibur or FACSAria instruments (BD Biosciences).

Statistical analysis

Quantitative data are presented as means ±SD and were analyzed with the 2-tailed Student *t* test. A P value of $< .05$ was considered statistically significant.

Additional procedures can be found in the supplemental data (available on the *Blood* web site; see the supplemental Materials link at the top of the online article).

Results

p57 deficiency in T cells results in developmental arrest at the DN3-DN4 transition

To investigate the role of p57 in T cell differentiation, we set out to delete the p57 gene specifically in T cells. Given that the *p57* locus undergoes genomic imprinting with only the maternal allele being expressed,[24] we crossed female mice heterozygous for a floxed allele ($p57^{[F]/+}$ or $p57^{[+]/F}$, with the symbols within square brackets representing the imprinted, inactive allele) with male mice harboring a *Cre* transgene under the control of the Lck gene promoter to yield Lck-Cre/$p57^{[+]/F}$ mice, in which the maternal *p57* allele would be expected to be deleted exclusively in the T cell lineage. We confirmed that the floxed allele was indeed efficiently inactivated by Cre in T cells of these mice (Figure 1A).

The size and cell number for the thymus of Lck-Cre/$p57^{[+]/F}$ mice were markedly reduced compared with those for control (Lck-Cre/$p57^{[+]/+}$) mice (Figure 1B-C). Although the size of the spleen in Lck-Cre/$p57^{[+]/F}$ mice did not differ substantially from that in control animals (Figure 1D), the number of TCRβ-positive cells in the spleen of the mutant mice was also reduced significantly compared with that in controls (Figure 1E). Flow cytometric analysis of the thymus of Lck-Cre/$p57^{[+]/F}$ mice showed an increased proportion of DN cells and a reduced percentage of DP cells (Figure 1F). Further analysis of CD44 and CD25 expression in the DN subset showed an increase in the proportion of DN3 cells accompanied by a marked decrease in that of DN4 cells (Figure 1G), indicating that the transition from DN3 to DN4 was blocked by p57 ablation. This differentiation block in DN3 cells also reduced the absolute numbers of cells at later stages of differentiation (DN4, ISP, DP, CD4, or CD8 SP) in the mutant mice (Figure 1H).

To investigate the mechanism by which p57 deficiency results in the differentiation block at the DN3-DN4 transition, we examined DNA rearrangement at the TCRβ locus and the expression of pre-TCR components in the DN3 cell population, given that an increase in the percentage of DN3 cells is often observed as a result of a defect in β-selection. Analysis of genomic DNA for DJβ and V(D)Jβ rearrangement in DN3 cells showed no substantial differences between Lck-Cre/$p57^{[+]/F}$ and Lck-Cre/$p57^{[+]/+}$ mice (Figure 1I), suggesting that the genomic rearrangement underlying TCRβ chain production is intact in the p57-deficient cells. The frequency of DN3 cells positive for intracellular TCRβ expression also did not differ significantly between the 2 genotypes (Figure 1J-K). However, the proportion of DN4 cells positive for intracellular TCRβ expression was greatly reduced by p57 ablation (Figure 1J-K), providing additional evidence that the differentiation of p57-deficient T cells is blocked at the DN3-DN4 transition. We also found that the abundance of pTα mRNA was increased in p57-deficient DN3 cells compared with control cells (Figure 1L), suggesting that the loss of p57 in immature T cells results in a reduction in the number of these cells without impairment of pre-TCR signaling.

Loss of p57 in immature T cells impairs proliferation and induces apoptosis in association with Rb hyperphosphorylation

Mice in which the gene encoding pTα is inactivated manifest a marked, but incomplete, block in T cell development at the transition from DN3 to DN4, as shown by a decrease in the proportion of proliferating DN4 cells.[25] Given that the timing of the differentiation block in p57-deficient T cells is almost identical to that in pTα-deficient mice, we examined the frequencies of proliferating cells and apoptotic cells among the DN3 and DN4 subsets in our mutant mice. Similar to the findings with pTα-deficient mice, the frequency of proliferating cells among the DN4 population of Lck-Cre/$p57^{[+]/F}$ mice was markedly decreased compared with that for control mice, whereas that for p57-deficient DN3 cells was reduced to a lesser extent (Figure 2A-B). Furthermore, we found that the frequency of apoptosis in DN4 cells was increased by p57 ablation (Figure 2C-D). These results suggested that a combination of cell cycle arrest and induction of apoptosis is responsible for the developmental defect in p57-deficient T cells. The sum of these effects of p57 deficiency thus

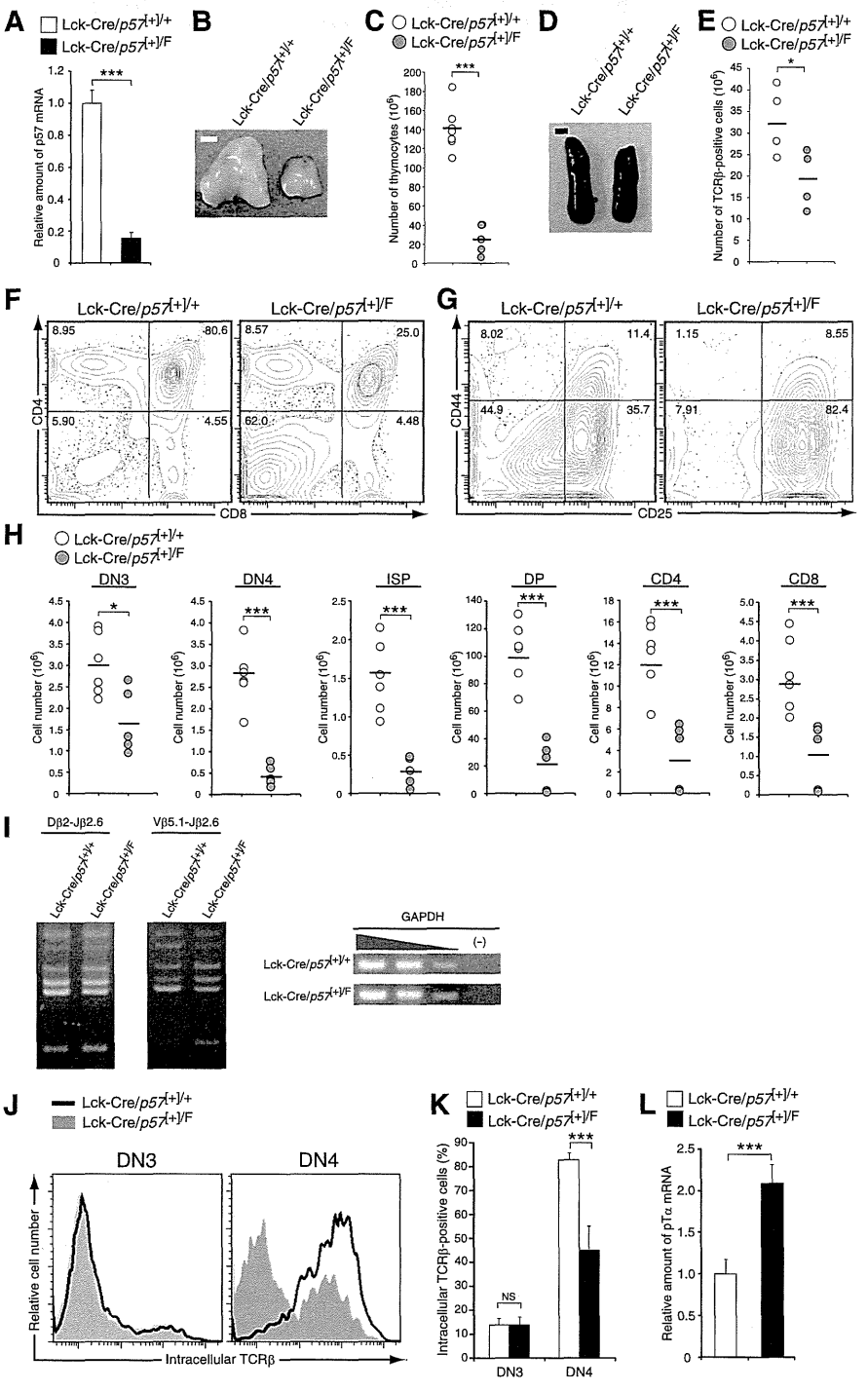

Figure 1. Loss of p57 in T cells results in a differentiation block at the DN3-DN4 transition and reduced thymic cellularity. (A) Reverse transcription (RT) and real-time PCR analysis of p57 mRNA in DN3 thymocytes from Lck-Cre/$p57^{[+]/+}$ and Lck-Cre/$p57^{[+]/F}$ mice at 8 weeks of age. Normalized data are expressed relative to the value for control mice and are means ±SD for 3 mice. ***$P < .005$. (B) Gross appearance of the thymus of Lck-Cre/$p57^{[+]/+}$ and Lck-Cre/$p57^{[+]/F}$ mice at 8 weeks of age. Bar, 2 mm. (C) Total number of thymocytes for individual Lck-Cre/$p57^{[+]/+}$ ($n = 7$) and Lck-Cre/$p57^{[+]/F}$ ($n = 5$) mice at 8 weeks of age. Bars indicate mean values. ***$P < .005$. (D) Gross appearance of the spleen of Lck-Cre/$p57^{[+]/+}$ and Lck-Cre/$p57^{[+]/F}$ mice at 8 weeks of age. Bar, 2 mm. (E) Number of TCRβ-positive cells among splenocytes of individual Lck-Cre/$p57^{[+]/+}$ and Lck-Cre/$p57^{[+]/F}$ mice at 8 weeks of age ($n = 4$). *$P < .05$. (F-G) Representative flow cytometric analysis of CD4 vs CD8 on thymocytes (F) and of CD44 vs CD25 on electronically gated lineage-negative DN thymocytes (G) from Lck-Cre/$p57^{[+]/+}$ and Lck-Cre/$p57^{[+]/F}$ mice at 8 weeks of age. Percentages of each fraction are indicated. (H) Absolute cell number for thymocyte subsets determined by flow cytometry ($n = 6$ for Lck-Cre/$p57^{[+]/+}$ and $n = 5$ for Lck-Cre/$p57^{[+]/F}$ mice). *$P < .05$, ***$P < .005$. (I) PCR analysis of genomic DNA for Dβ-to-Jβ rearrangement or V(D)Jβ recombination in DN3 cells from Lck-Cre/$p57^{[+]/+}$ and Lck-Cre/$p57^{[+]/F}$ mice at 8 weeks of age. Amplification of a GAPDH gene fragment was performed as an input control. (J) Representative histograms for flow cytometric analysis of intracellular TCRβ expression in DN3 and DN4 thymocytes from Lck-Cre/$p57^{[+]/+}$ and Lck-Cre/$p57^{[+]/F}$ mice at 8 weeks of age. (K) Determination of the proportion of cells positive for intracellular TCRβ expression as in panel J. Data are means ±SD for 4 mice. ***$P < .005$; NS, not significant. (L) RT and real-time PCR analysis of pTα mRNA in DN3 thymocytes from Lck-Cre/$p57^{[+]/+}$ and Lck-Cre/$p57^{[+]/F}$ mice at 8 weeks of age. Normalized data are expressed relative to the value for control mice and are means ±SD for 3 mice. ***$P < .005$.

likely accounts for the ~85% decrease in the number of DN4 cells in the mutant mice (Figure 1H).

We next investigated whether the Rb-E2F pathway is activated in p57-deficient T cells. Immunoblot (IB) analysis showed that the extent of Rb phosphorylation on Ser^{780} was increased in p57-deficient DN3 cells compared with control cells, whereas the extent of Rb phosphorylation at $Ser^{807/811}$ did not differ substantially between the 2 genotypes (Figure 2E). Examination of the expression of E2F target genes revealed that the expression levels of the genes for Mcm3, Cdc6, and Cdt1, all of which are related to cell cycle progression, were significantly increased in p57-deficient DN3 cells (Figure 2F). In addition, expression of the genes for ATM and ASPP1, which are E2F targets involved in apoptosis, was also markedly increased in these cells (Figure 2G). These results thus indicated that E2F activity was indeed increased by ablation of p57 in T cells.

p57 is not required for T cell development at the DP stage

We next examined whether p57 is also indispensable for the development of mature T cells. To bypass the requirement for p57 at the earlier stage of T cell development, we crossed p57-floxed mice

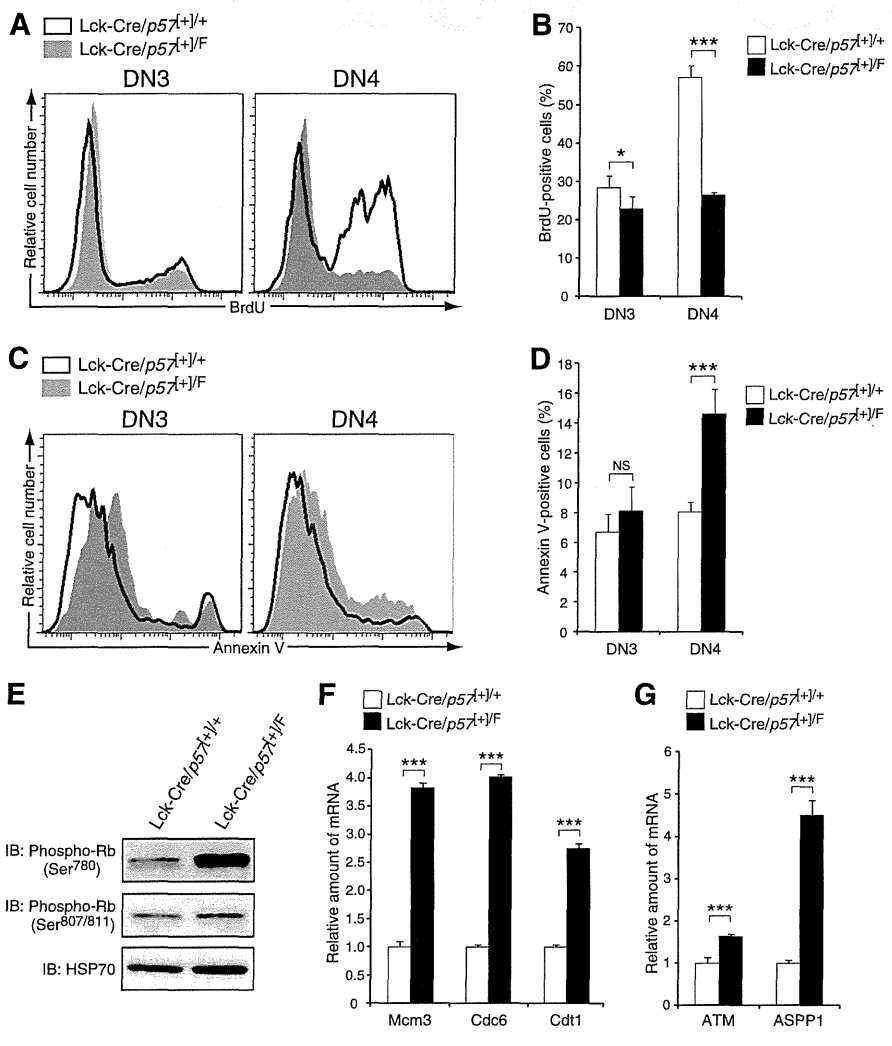

Figure 2. Loss of p57 results in a proliferative defect, induction of apoptosis, and excessive phosphorylation of Rb in thymocytes. (A) Representative flow cytometric histograms for BrdU staining in DN3 and DN4 thymocytes from Lck-Cre/$p57^{[+]/+}$ and Lck-Cre/$p57^{[+]/F}$ mice injected with BrdU at 8 weeks of age. (B) Determination of the proportion of cells positive for BrdU as in panel A. Data are means ±SD for 4 mice. $^{*}P < .05$, $^{***}P < .005$. (C) Representative histograms for annexin V staining in DN3 and DN4 thymocytes from Lck-Cre/$p57^{[+]/+}$ and Lck-Cre/$p57^{[+]/F}$ mice at 8 weeks of age. (D) Determination of the proportion of cells positive for annexin V staining as in panel C. Data are means ±SD for 4 mice. $^{***}P < .005$. (E) IB analysis of phosphorylated Rb in DN3 thymocytes from Lck-Cre/$p57^{[+]/+}$ and Lck-Cre/$p57^{[+]/F}$ mice at 8 weeks of age. HSP70 was examined as a loading control. (F-G) RT and real-time PCR analysis of Mcm3, Cdc6, and Cdt1 mRNAs (F) as well as of ATM and ASPP1 mRNAs (G) in DN3 thymocytes from Lck-Cre/$p57^{[+]/+}$ and Lck-Cre/$p57^{[+]/F}$ mice at 8 weeks of age. Normalized data are expressed relative to the corresponding value for control mice and are means ±SD for 3 mice. $^{***}P < .005$.

with CD4-Cre transgenic mice to generate CD4-Cre/$p57^{[+]/F}$ mice. Cre recombinase is not expressed in thymocytes of CD4-Cre mice until the late stage of DN cell development,[23] and consistent with this we detected a significant decrease in the abundance of p57 mRNA in DN4 cells but not in DN3 cells from CD4-Cre/$p57^{[+]/F}$ mice (Figure 3A). The size of the thymus and number of thymocytes did not differ between these mutant mice and control animals (Figure 3B-C). The numbers of DN3, DN4, DP, CD4 SP, and CD8 SP cells in CD4-Cre/$p57^{[+]/F}$ mice were also similar to those in control littermates, whereas the number of ISP cells was increased in the mutant animals (Figure 3D-E). These results thus indicated that p57 is dispensable for T cell development after the DP stage.

p57-deficient mature T cells proliferate inefficiently in response to antigenic stimulation

Although the number of T cells in the thymus of CD4-Cre/$p57^{[+]/F}$ mice did not differ significantly from that for control mice, the number of TCRβ-positive cells in the spleen of CD4-Cre/$p57^{[+]/F}$ mice was significantly reduced (Figure 3F). To investigate the mechanism underlying this phenotype, we first examined BrdU incorporation and apoptosis in splenic T cells after mitogenic stimulation. The extent of BrdU incorporation was attenuated in splenic T cells from CD4-Cre/$p57^{[+]/F}$ mice at 36 hours after the onset of stimulation with antibodies to CD3ε (Figure 3G). Furthermore, the frequency of apoptotic cells was increased in splenic T cells from CD4-Cre/$p57^{[+]/F}$ mice after stimulation for 24 or 36 hours (Figure 3H). These results thus suggested that p57 is indispensable for the continuous proliferation of mature T cells in response to mitogenic stimulation, which is necessary for maintenance of the T cell population in peripheral lymphoid organs.

We next examined the possible contribution of the Rb-E2F pathway to the impaired proliferation of mature T cells from CD4-Cre/$p57^{[+]/F}$ mice. Whereas the extent of Rb phosphorylation on Ser^{780} was not greatly increased by p57 ablation in the absence or presence of anti-CD3ε stimulation, the extent of that at $Ser^{807/811}$ was increased in splenic T cells from CD4-Cre/$p57^{[+]/F}$ mice under both conditions (Figure 3I). This pattern of Rb phosphorylation on $Ser^{807/811}$ and Ser^{780} is opposite to that apparent for p57-deficient immature T cells (Figure 2E). In addition, the expression levels of the genes for Cdc6 and Cdt1 were significantly increased in the p57-deficient mature T cells, although those for the Mcm3, ATM, and ASPP1 genes did not differ between the 2 genotypes (Figure 3J-K). This pattern of E2F target gene expression differs from that apparent in thymocytes (Figure 2F-G), possibly as a result of the difference in the sites of Rb phosphorylation. Collectively, our data suggested that the reduction in the number of TCRβ-positive cells in the spleen of CD4-Cre/$p57^{[+]/F}$ mice is attributable, at least in part, to excessive activation of the Rb-E2F pathway in

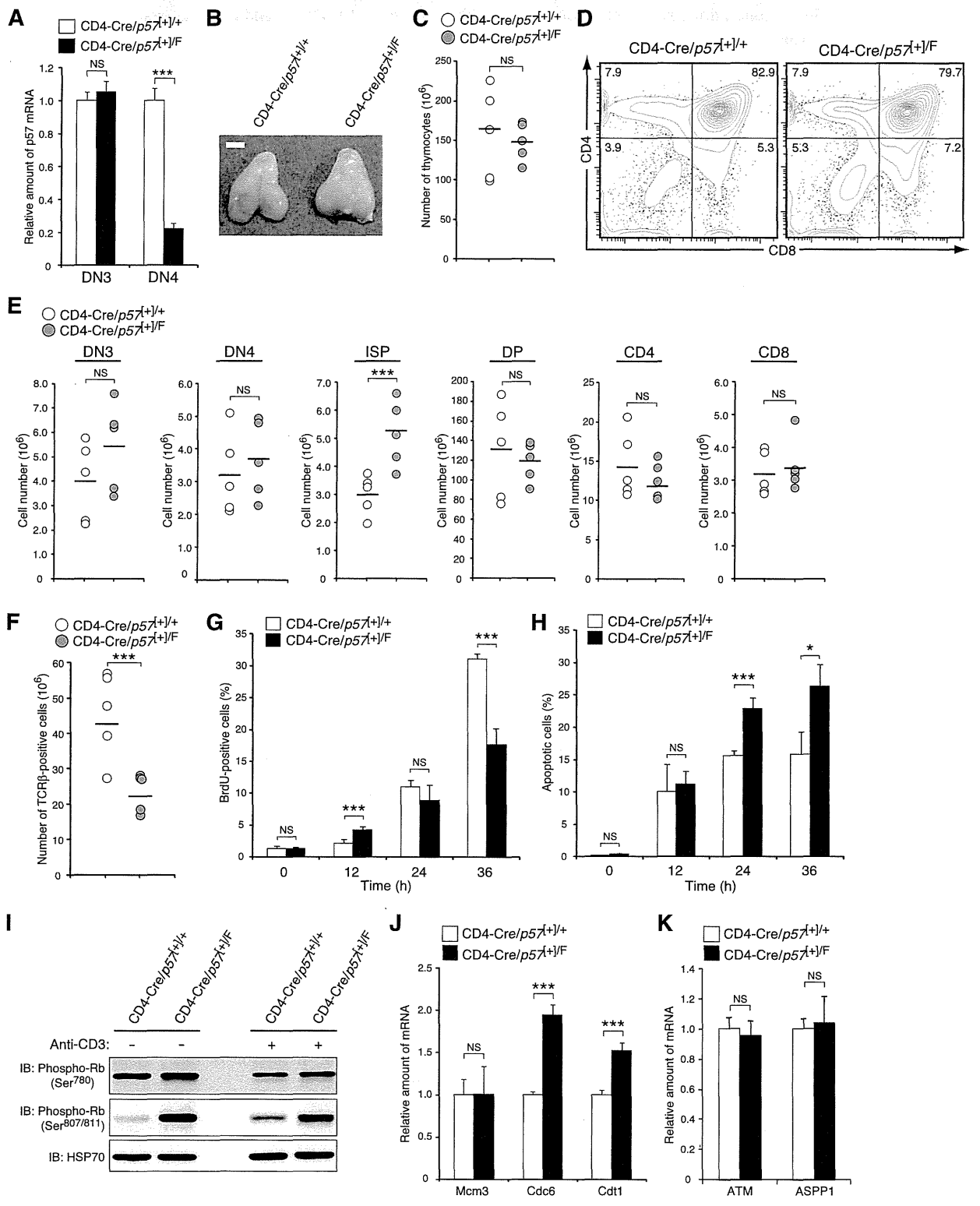

Figure 3. Ablation of p57 does not affect development of DP cells but impairs the proliferation and survival of antigen-stimulated mature T cells. (A) RT and real-time PCR analysis of p57 mRNA in DN3 and DN4 thymocytes from CD4-Cre/$p57^{[+]/+}$ and CD4-Cre/$p57^{[+]/F}$ mice at 8 weeks of age. Normalized data are expressed relative to the corresponding value for control mice and are means ±SD for 3 mice. ***$P < .005$. (B) Gross appearance of the thymus of CD4-Cre/$p57^{[+]/+}$ and CD4-Cre/$p57^{[+]/F}$ mice at 8 weeks of age. Bar, 2 mm. (C) Total number of thymocytes for individual CD4-Cre/$p57^{[+]/+}$ and CD4-Cre/$p57^{[+]/F}$ mice at 8 weeks of age ($n = 5$). (D) Representative flow cytometric analysis of CD4 vs CD8 on thymocytes from CD4-Cre/$p57^{[+]/+}$ and CD4-Cre/$p57^{[+]/F}$ mice at 8 weeks of age. Percentages of each fraction are indicated. (E) Absolute cell number for thymocyte subsets in individual CD4-Cre/$p57^{[+]/+}$ and CD4-Cre/$p57^{[+]/F}$ mice at 8 weeks of age ($n = 5$). ***$P < .005$. (F) Absolute number of TCRβ-positive cells among splenocytes from individual CD4-Cre/$p57^{[+]/+}$ and CD4-Cre/$p57^{[+]/F}$ mice at 8 weeks of age ($n = 5$). ***$P < .005$. (G) Splenic $CD3^+$ T cells from CD4-Cre/$p57^{[+]/+}$ and CD4-Cre/$p57^{[+]/F}$ mice at 8 weeks of age were stimulated with anti-CD3ε (5 μg/mL) for the indicated times and exposed to BrdU during the final 1 hour of incubation. They were then stained with anti-BrdU, and the percentage of BrdU-positive cells was determined by flow cytometry. Data are means ±SD for 3 mice. ***$P < .005$. (H) Splenic T cells stimulated as in panel G were stained with propidium iodide, and the percentage of sub-G_1 (apoptotic) cells was determined by flow cytometry. Data are means ±SD for 3 mice. *$P < .05$, ***$P < .005$. (I) IB analysis of phosphorylated Rb in splenic T cells stimulated (or not) as in panel G for 10 hours. (J-K) RT and real-time PCR analysis of Mcm3, Cdc6, and Cdt1 mRNAs (J) as well as of ATM and ASPP1 mRNAs (K) in splenic T cells stimulated as in panel G for 10 hours. Normalized data are expressed relative to the corresponding value for control mice and are means ±SD for 3 mice. ***$P < .005$.

response to antigenic stimulation and the resultant induction of apoptosis and cell cycle arrest.

Additional ablation of E2F1 attenuates the defects of p57-deficient T cells

Our results indicated that E2F activity is increased in both immature and mature T cells by ablation of p57. To examine whether the defects of p57-deficient T cells are indeed attributable to this activation of E2F, we crossed Lck-Cre/$p57^{[+]/F}$ mice with $E2f1^{-/-}$ mice to generate animals that lack both p57 and E2F1 in T cells. The decreases in the size of the thymus and the number of thymocytes in Lck-Cre/$p57^{[+]/F}$ mice were partially reversed by additional ablation of E2F1 (Figure 4A-B). Flow cytometric analysis showed that E2F1 ablation also resulted in a partial rescue of the increase in the frequency of DN3 cells in Lck-Cre/$p57^{[+]/F}$ mice (Figure 4C-D). This attenuation of the differentiation block at the DN3-DN4 transition led to a partial recovery of the absolute cell numbers of each thymocyte compartment in the p57/E2F1 double-mutant mice (Figure 4E).

In comparison with the partial rescue of defects apparent in p57-deficient thymocytes, additional E2F1 ablation almost completely reversed those in p57-deficient splenic T cells. The number of TCRβ-positive cells in the spleen of Lck-Cre/$p57^{[+]/F}$ mice was thus restored to almost the same level as that of control animals by E2F1 ablation (Figure 4F). In addition, E2F1 deficiency completely reversed the changes in the extent of mitogen-induced BrdU incorporation and apoptosis in splenic T cells from Lck-Cre/$p57^{[+]/F}$ mice compared with those from control mice (Figure 4G-H). These results thus indicated that activation of the E2F pathway indeed contributes to the phenotypes of both p57-deficient immature and mature T cells and that the dependency of these phenotypes on such activation is greater in mature T cells than in immature T cells.

Additional ablation of p53 attenuates the phenotypes of p57 deficiency in immature but not mature T cells

Excessive activation of E2F was previously shown to induce p53-dependent or p53-independent apoptosis in a manner dependent on cellular context.[10-13] Indeed, the abundance of mRNAs for p21, Noxa, and Bax, all of which are downstream targets of p53, was increased in DN3 cells of Lck-Cre/$p57^{[+]/F}$ mice (Figure 5A). Furthermore, the abundance of all 3 mRNAs in DN3 cells of Lck-Cre/$p57^{[+]/F}$/$E2f1^{-/-}$ mice was reduced compared with that for DN3 cells of Lck-Cre/$p57^{[+]/F}$ mice (Figure 5A), although this reversal of p53 activation by E2F1 ablation was only partial. We therefore next crossed Lck-Cre/$p57^{[+]/F}$ mice with $p53^{-/-}$ mice to generate animals that lack both p57 and p53 in T cells. The size of the thymus in Lck-Cre/$p57^{[+]/F}$/$p53^{-/-}$ mice was indistinguishable from that in control mice, and we did not detect an increase in the frequency of DN3 cells in the double-mutant animals (Figure 5B-D). The cell numbers for each thymocyte subset in Lck-Cre/$p57^{[+]/F}$ mice were also completely recovered by additional p53 ablation; in particular, the number of ISP cells in Lck-Cre/$p57^{[+]/F}$/$p53^{-/-}$ mice exceeded that in controls (Figure 5E). Collectively, these results suggested that the differentiation block at the DN3-DN4 transition induced by p57 loss is attributable to hyperactivation of p53.

We next examined whether p53 hyperactivation is also responsible for the defects of p57-deficient mature T cells. Whereas the decrease in the number of TCRβ-positive cells in the spleen of Lck-Cre/$p57^{[+]/F}$ mice was completely reversed by the additional ablation of E2F1 (Figure 4F), the ablation of p53 did not reproduce this effect (Figure 6A). Consistent with this result, the abundance of mRNAs for p53 target genes, including those for p21, Noxa, and Bax, was not increased in splenic T cells of Lck-Cre/$p57^{[+]/F}$ mice compared with those of control animals in the absence or presence of anti-CD3ε stimulation (Figure 6B). We also measured BrdU incorporation and the frequency of apoptosis after mitogenic stimulation, and found that additional depletion of p53 did not affect the phenotypes of p57-deficient splenic T cells (Figure 6C-D). Together, these results suggested that, in contrast to immature T cells, the induction of apoptosis and cell cycle arrest by p57 loss in mature T cells are p53 independent.

Given that activated E2F1 was previously shown to increase transcription of the caspase-8 and Bid genes, as well as to enhance Fas signaling in mature T cells,[26] such effects might underlie the increased level of apoptosis in p57-deficient mature T cells. We therefore measured the abundance of mRNAs for caspase-8 and Bid in splenic $CD3^+$ T cells from Lck-Cre/$p57^{[+]/+}$ and Lck-Cre/$p57^{[+]/F}$ mice with or without anti-CD3ε stimulation. We found that the amounts of these mRNAs were indeed increased in $CD3^+$ T cells of Lck-Cre/$p57^{[+]/F}$ mice compared with the control cells after anti-CD3ε stimulation (Figure 6E), suggesting that the caspase-8–Bid pathway contributes to the phenotypes of p57-deficient mature T cells.

Loss of p57 predisposes immature T cells to thymic lymphoma

Given that our data suggested that p53 suppresses aberrant expansion of p57-deficient immature T cells, we examined whether the simultaneous loss of p57 and p53 might eventually result in tumorigenesis. At 8 weeks of age, some of Lck-Cre/$p57^{[+]/F}$/$p53^{-/-}$ mice indeed developed aggressive lymphomas characterized by massive thymic enlargement (Figure 7A). In Figure 7A, 1 of the fastest developing lymphomas in Lck-Cre/$p57^{[+]/F}$/$p53^{-/-}$ mice is shown. Flow cytometric analysis showed a marked increase in the size of the ISP cell population in the Lck-Cre/$p57^{[+]/F}$/$p53^{-/-}$ mice (Figure 7B-C). All of the double-mutant mice died between 14 and 24 weeks of age, indicating that the lymphomas were fatal. Comparison of the timing of thymic lymphoma development demonstrated that the p57/p53 double-mutant mice developed this condition with a reduced latency compared with $p53^{-/-}$ mice, and that Lck-Cre/$p57^{[+]/F}$/$p53^{+/-}$ mice also exhibited a markedly reduced viability compared with $p53^{+/-}$ mice (Figure 7D). None of 13 Lck-Cre/$p57^{[+]/F}$ mice developed lymphoma for up to 500 days of age, supporting the notion that p53 suppresses aberrant expansion of p57-deficient T cells. We thus concluded that p57 and p53 cooperatively prevent excessive proliferation of T cells in the thymus and that disruption of this p57-p53 axis results in lymphomagenesis.

Discussion

Previous studies have indicated that the differentiation of DN3 cells into DN4 cells depends on the balance between p53 activity and pre-TCR signaling (Figure 7E upper left).[4-6] Mice deficient in RAG1/2, DNA-PK, or CD3γ thus exhibit a differentiation block at the DN3 to DN4 stages that is attributable to impaired formation of the pre-TCR complex and consequent abrogation of pre-TCR signaling (Figure 7E upper center). On the other hand, mice deficient in p53 often develop lymphoma,[27] supporting the notion that p53 activity is required for appropriate T cell development (Figure 7E upper

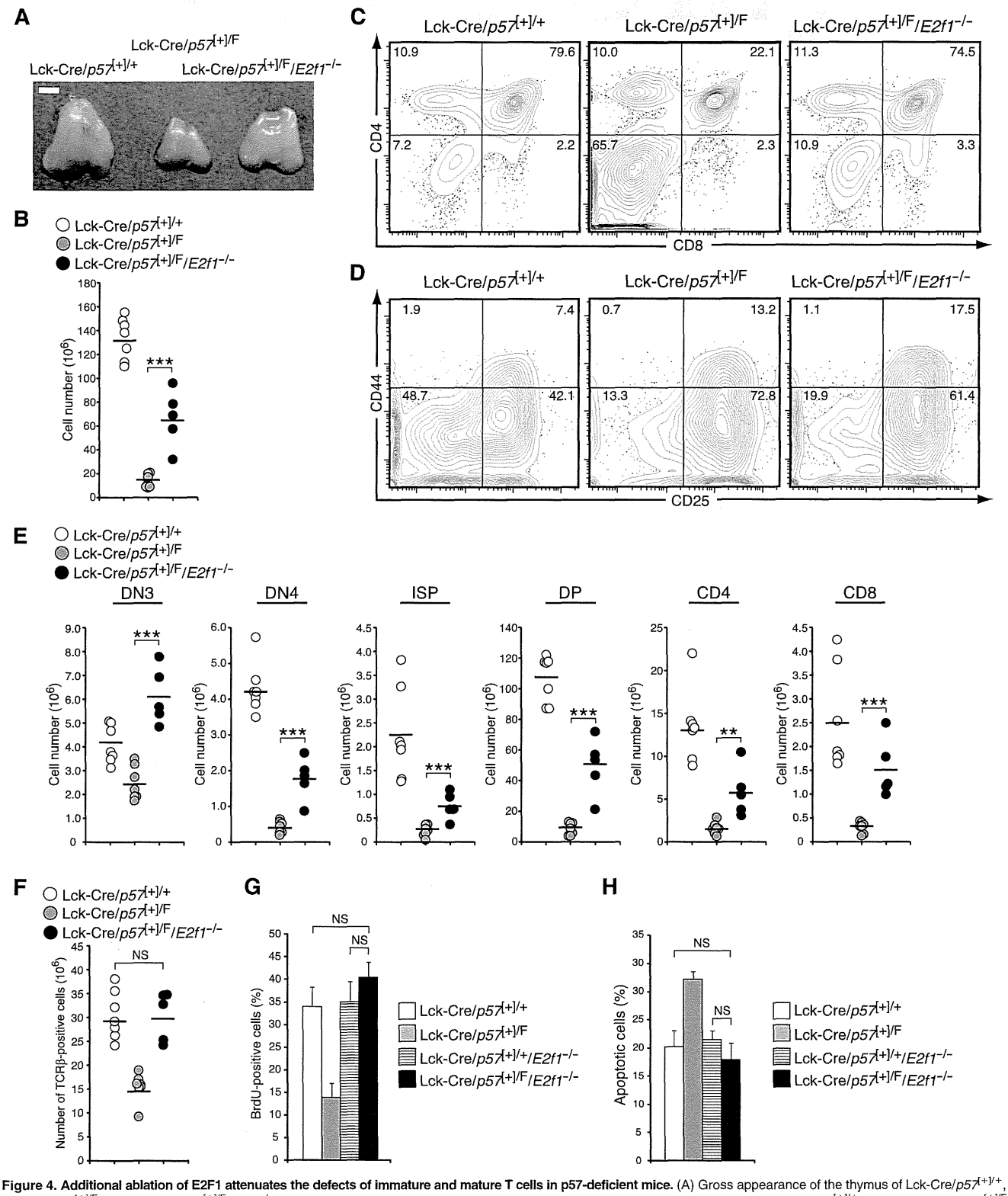

Figure 4. Additional ablation of E2F1 attenuates the defects of immature and mature T cells in p57-deficient mice. (A) Gross appearance of the thymus of Lck-Cre/$p57^{[+]/+}$, Lck-Cre/$p57^{[+]/F}$, and Lck-Cre/$p57^{[+]/F}$/$E2f1^{-/-}$ mice at 8 weeks of age. Bar, 2 mm. (B) Total number of thymocytes for individual Lck-Cre/$p57^{[+]/+}$ ($n = 7$), Lck-Cre/$p57^{[+]/F}$ ($n = 7$), and Lck-Cre/$p57^{[+]/F}$/$E2f1^{-/-}$ ($n = 5$) mice at 8 weeks of age. ***$P < .005$. (C-D) Representative flow cytometric analysis of CD4 vs CD8 on thymocytes (C) as well as of CD44 vs CD25 on electronically gated lineage-negative DN thymocytes (D) from Lck-Cre/$p57^{[+]/+}$, Lck-Cre/$p57^{[+]/F}$, and Lck-Cre/$p57^{[+]/F}$/$E2f1^{-/-}$ mice at 8 weeks of age. Percentages of each fraction are indicated. (E) Absolute cell number for thymocyte subsets from individual Lck-Cre/$p57^{[+]/+}$ ($n = 7$), Lck-Cre/$p57^{[+]/F}$ ($n = 7$), and Lck-Cre/$p57^{[+]/F}$/$E2f1^{-/-}$ ($n = 5$) mice at 8 weeks of age determined by flow cytometry. **$P < .01$, ***$P < .005$. (F) Number of TCRβ-positive cells among splenocytes from individual Lck-Cre/$p57^{[+]/+}$ ($n = 7$), Lck-Cre/$p57^{[+]/F}$ ($n = 7$), and Lck-Cre/$p57^{[+]/F}$/$E2f1^{-/-}$ ($n = 5$) mice at 8 weeks of age. (G-H) Splenic $CD3^+$ T cells from mice of the indicated genotypes at 8 weeks of age were stimulated with anti-CD3ε (5 μg/mL) for 36 hours and exposed to BrdU during the final 1 hour of incubation. They were then stained with anti-BrdU and propidium iodide, and the percentages of BrdU-positive cells (G) and of sub-G_1 (apoptotic) cells (H) were determined by flow cytometry. Data are means ±SD for 3 mice.

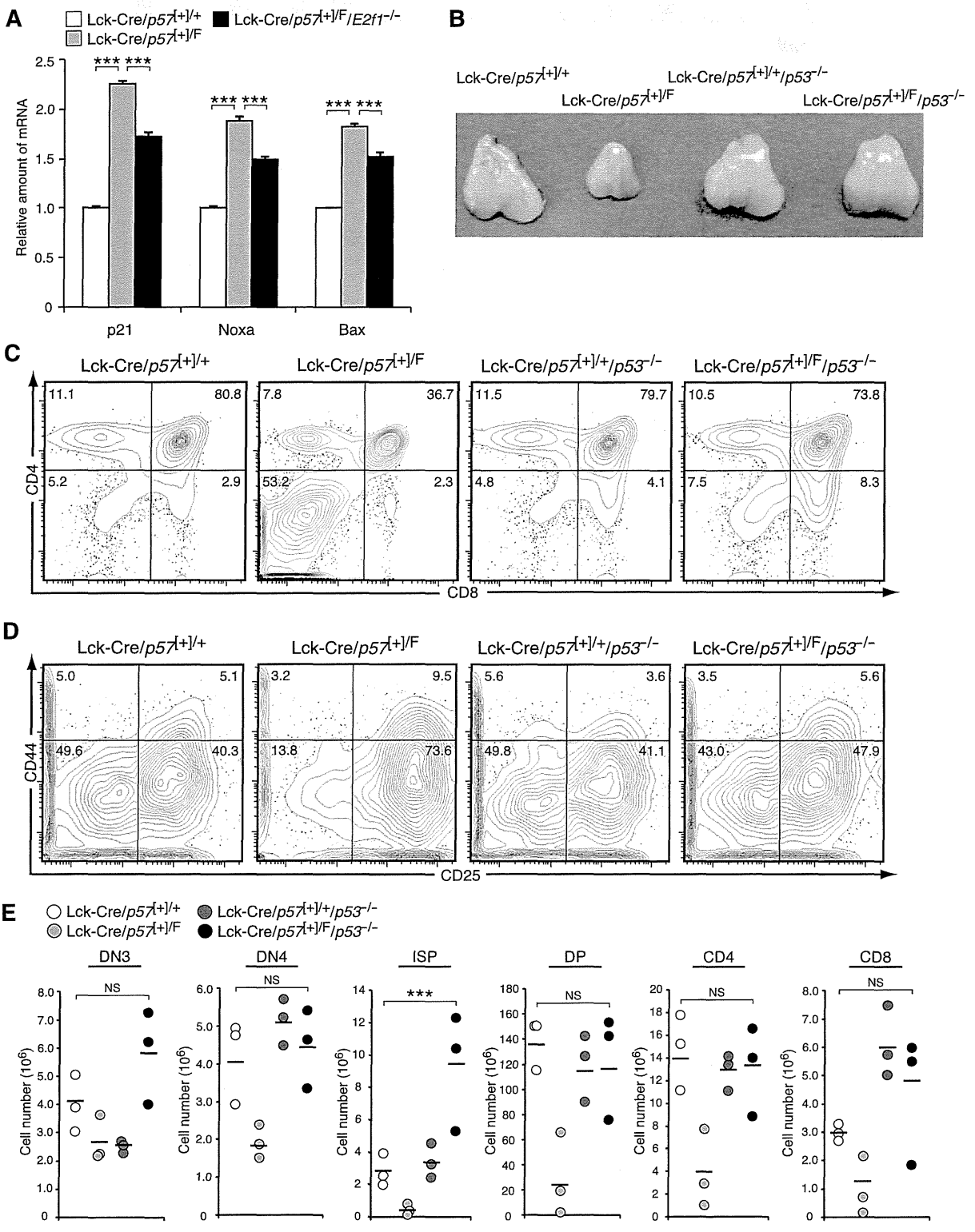

Figure 5. The pre-T cell differentiation block in p57-deficient mice is overcome by additional ablation of p53. (A) RT and real-time PCR analysis of p21, Noxa, and Bax mRNAs in DN3 thymocytes from Lck-Cre/$p57^{[+]/+}$, Lck-Cre/$p57^{[+]/F}$, and Lck-Cre/$p57^{[+]/F}$/$E2f1^{-/-}$ mice at 8 weeks of age. Normalized data are expressed relative to the corresponding value for control mice and are means ±SD for 3 mice. ***$P < .005$. (B) Gross appearance of the thymus of Lck-Cre/$p57^{[+]/+}$, Lck-Cre/$p57^{[+]/F}$, Lck-Cre/$p57^{[+]/+}$/$p53^{-/-}$, and Lck-Cre/$p57^{[+]/F}$/$p53^{-/-}$ mice at 7 weeks of age. Bar, 2 mm. (C-D) Representative flow cytometric analysis of CD4 vs CD8 on thymocytes (C) as well as of CD44 vs CD25 on electronically gated lineage-negative DN thymocytes (D) from Lck-Cre/$p57^{[+]/+}$, Lck-Cre/$p57^{[+]/F}$, Lck-Cre/$p57^{[+]/+}$/$p53^{-/-}$, and Lck-Cre/$p57^{[+]/F}$/$p53^{-/-}$ mice at 7 weeks of age. Percentages of each fraction are indicated. (E) Absolute cell numbers determined by flow cytometry for thymocyte subsets from individual Lck-Cre/$p57^{[+]/+}$, Lck-Cre/$p57^{[+]/F}$, Lck-Cre/$p57^{[+]/+}$/$p53^{-/-}$, and Lck-Cre/$p57^{[+]/F}$/$p53^{-/-}$ mice at 7 weeks of age ($n = 3$). ***$P < .005$.

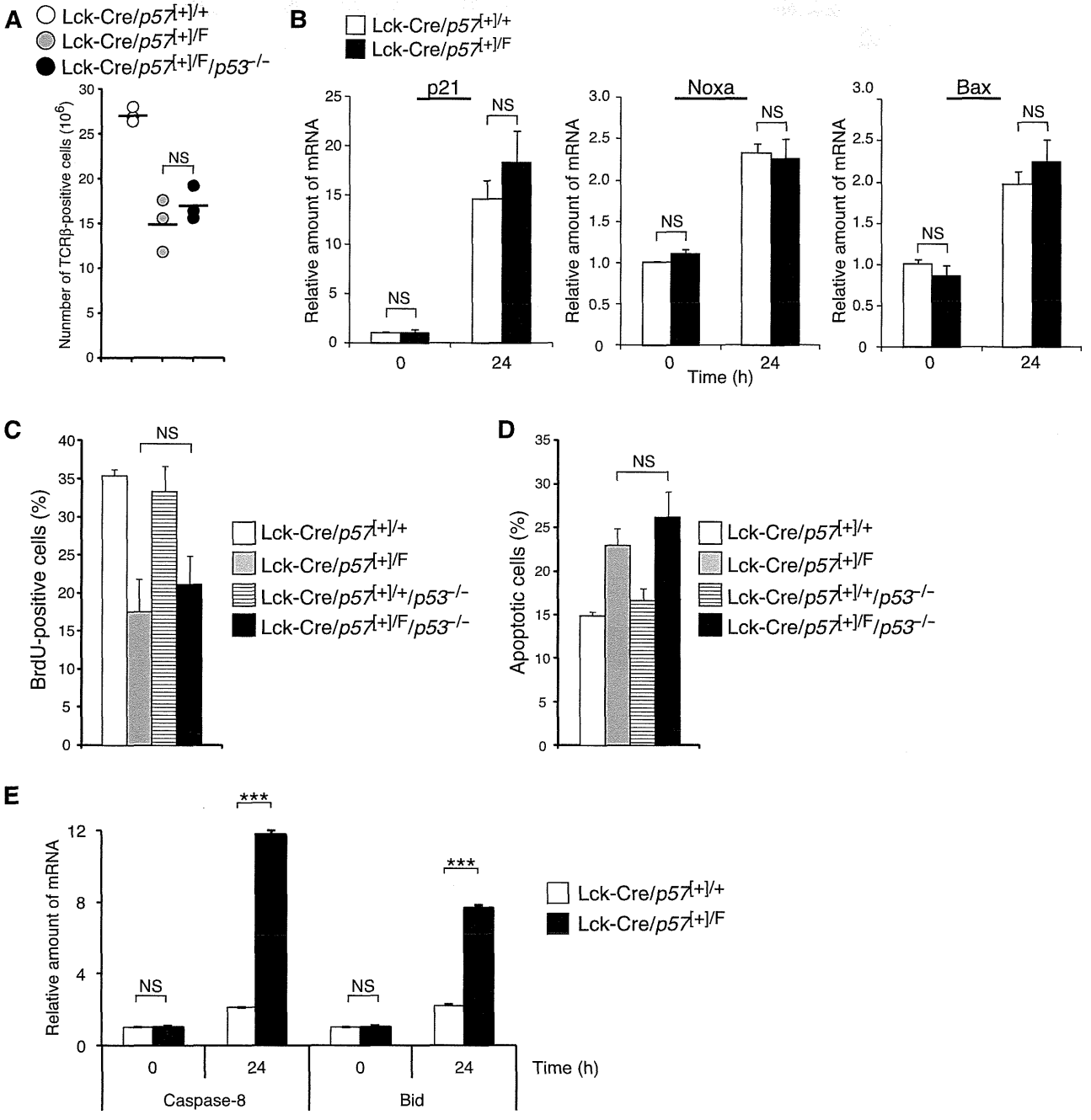

Figure 6. The proliferation and survival defects of mature T cells from p57-deficient mice are not rescued by additional ablation of p53. (A) Number of TCRβ-positive cells among splenocytes from individual Lck-Cre/$p57^{[+]/+}$, Lck-Cre/$p57^{[+]/F}$, and Lck-Cre/$p57^{[+]/F}/p53^{-/-}$ mice at 7 weeks of age ($n = 3$). (B) Splenic $CD3^+$ T cells from Lck-Cre/$p57^{[+]/+}$ and Lck-Cre/$p57^{[+]/F}$ mice at 8 weeks of age were stimulated with anti-CD3ε (5 μg/mL) for the indicated times, after which the abundance of p21, Noxa, and Bax mRNAs was determined by RT and real-time PCR analysis. Normalized data are expressed relative to the corresponding value for cells from control mice at time 0 and are means ±SD for 3 mice. (C-D) Splenic $CD3^+$ T cells from Lck-Cre/$p57^{[+]/+}$, Lck-Cre/$p57^{[+]/F}$, Lck-Cre/$p57^{[+]/+}/p53^{-/-}$, and Lck-Cre/$p57^{[+]/F}/p53^{-/-}$ mice at 7 weeks of age were stimulated with anti-CD3ε for 36 hours and exposed to BrdU during the final 1 hour of incubation. They were then stained with anti-BrdU and propidium iodide, and the percentages of BrdU-positive cells (C) and of sub-G_1 (apoptotic) cells (D) were determined by flow cytometry. Data are means ±SD for 3 mice. (E) Splenic $CD3^+$ T cells from Lck-Cre/$p57^{[+]/+}$ and Lck-Cre/$p57^{[+]/F}$ mice at 8 weeks of age were stimulated as in panel B, after which the abundance of caspase-8 and Bid mRNAs was determined by RT and real-time PCR analysis. Normalized data are expressed relative to the corresponding value for cells from control mice at time 0 and are means ±SD for 3 mice. ***$P < .005$.

right). We have now shown that ablation of p57 induces p53 hyperactivation as a result of upregulation of E2F activity in thymocytes. Whereas genomic rearrangement at the TCRβ locus and intracellular expression of TCRβ in p57-deficient DN3 cells were indistinguishable from those in control cells, the abundance of pTα mRNA was increased in the p57-deficient DN3 cells, suggesting that the extent of pre-TCR signaling was also increased in these cells (Figure 7E lower left). However, p53 hyperactivation dominates this increased level of pre-TCR signaling, leading to a differentiation block at the DN3-DN4 transition.

Whereas additional ablation of E2F1 completely rescued the phenotypes of p57-deficient splenic T cells, the reversal of those of

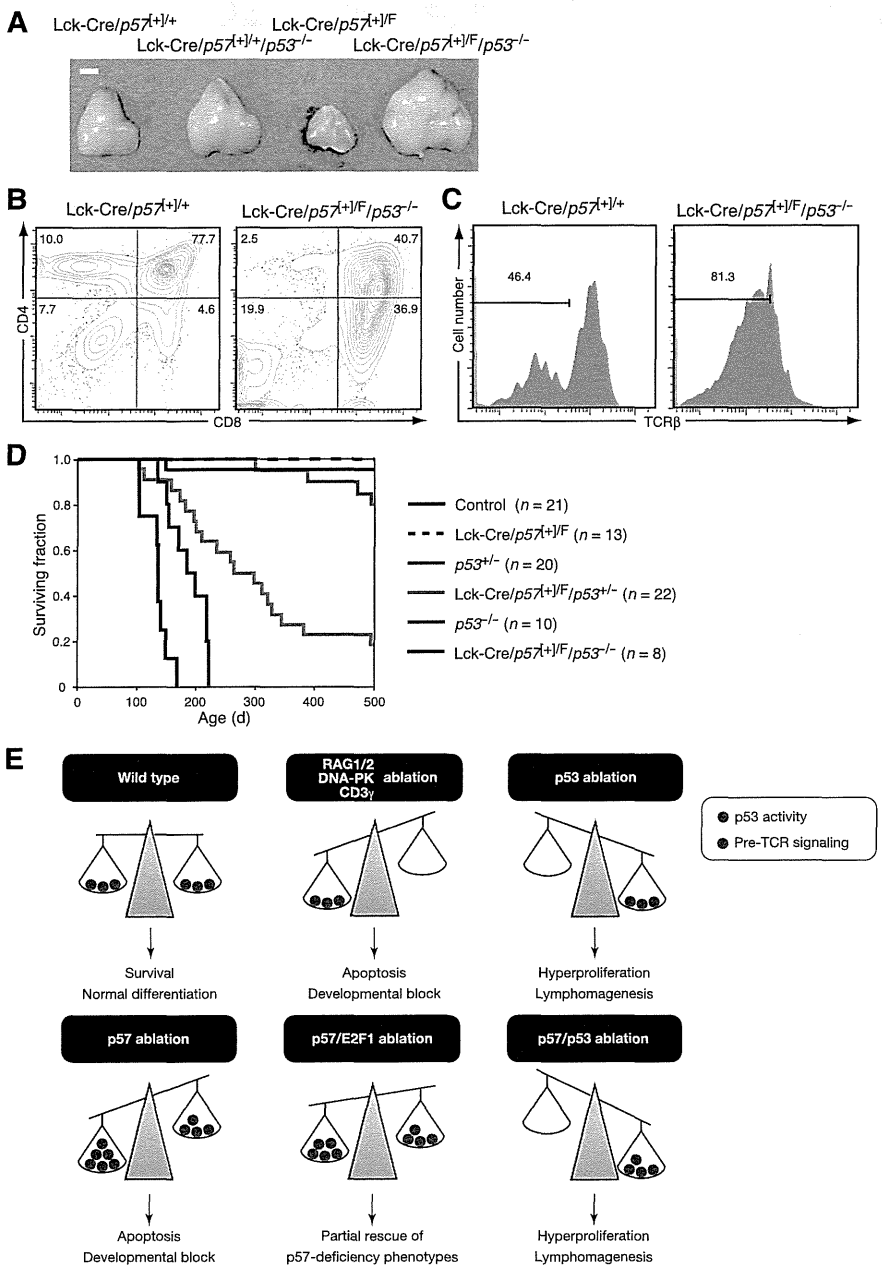

Figure 7. Mice lacking both p57 and p53 develop lymphoma. (A) Gross appearance of the thymus of Lck-Cre/$p57^{[+]/+}$, Lck-Cre/$p57^{[+]/+}/p53^{-/-}$, Lck-Cre/$p57^{[+]/F}$, and Lck-Cre/$p57^{[+]/F}/p53^{-/-}$ mice at 8 weeks of age. Bar, 2 mm. (B-C) Representative flow cytometric analysis of CD4 vs CD8 on thymocytes (B) as well as of TCRβ on electronically gated CD8 SP cells (C) from Lck-Cre/$p57^{[+]/+}$ and Lck-Cre/$p57^{[+]/F}/p53^{-/-}$ mice shown in panel A. Percentages of each fraction are indicated. (D) Kaplan-Meier plot for overall survival of mice of the indicated genotypes. (E) Model for the role of p57 in T cell differentiation and prevention of lymphomagenesis. Differentiation of pre-T cells depends on a balance between p53 activity and pre-TCR signaling. Ablation of p57 results in hyperactivation of p53 and thereby induces apoptosis in and blocks the development of immature T cells. Additional ablation of E2F1 results in a partial rescue of the phenotypes associated with p57 deficiency. The simultaneous ablation of p57 and p53 results in aberrant expansion of immature T cells, eventually leading to the development of fatal thymic lymphoma. See Discussion for further details.

p57-deficient immature T cells by E2F1 ablation was partial (Figure 7E lower center). Given that previous studies indicate that other members of the E2F family, such as E2F2 or E2F3, also contribute to the maturation of immature T cells,[28] activation of these other family members might be involved in the phenotypes of p57-deficient immature T cells.

Activated E2F promotes cell cycle progression by increasing the transcription of genes that contribute to the G_1-S transition.[8] E2F also promotes transcription of apoptosis-related genes, including those for ATM and ASPP1 that induce apoptosis through activation of p53.[29,30] Consistent with these findings, we found that the amounts of ATM and ASPP1 mRNAs as well as those of mRNAs derived from p53 target genes were increased in p57-deficient immature T cells in association with an increase in the frequency of apoptosis (Figure 7E lower left). Furthermore, additional ablation of p53 rescued p57-deficiency phenotypes in immature T cells, suggesting that the reduction in the number of these cells elicited by p57 ablation is attributable to p53-dependent cell cycle arrest and induction of apoptosis. Our data show that the predominant response to p53 activation in p57-deficient immature T cells is cell cycle arrest, although the mechanism by which a cell selects cell cycle arrest or apoptosis as the appropriate response to p53 activation remains elusive.

We found that the number of ISP cells in CD4-Cre/$p57^{[+]/F}$ mice and Lck-Cre/$p57^{[+]/F}/p53^{-/-}$ mice is even greater than that in corresponding control mice (Figures 3E and 5E), suggesting that loss of p57 may promote E2F-driven cell proliferation in ISP cells to a greater extent than in other T cell fractions. Consistent with this notion, p57/p53 double-mutant mice eventually develop fatal thymic lymphomas characterized by accumulation of ISP cells (Figure 7E lower right). Ablation of p57 alone did not confer an increased susceptibility to lymphoma development, suggesting that p53

suppresses such development in the context of p57 deficiency. In conclusion, our study has unveiled the physiological importance of the p57-E2F-p53 pathway in the proper development of T cells as well as in the prevention of lymphomagenesis, with our results providing the basis for a new paradigm in the relation between CDK inhibitors, development of the immune system, and lymphomagenesis.

Acknowledgments

The authors thank C. B. Wilson for CD4-Cre mice, L. Yamasaki for *E2f1*$^{-/-}$ mice, A. Niihara, C. Mitai, and M. Tanaka for technical assistance, and members of our laboratory for comments on the manuscript.

Authorship

Contribution: A.M. and S.T. performed experiments and wrote the manuscript; and K.I.N. designed research, interpreted data, and wrote the manuscript.

Conflict-of-interest disclosure: The authors declare no competing financial interests.

The current affiliation for A.M. is the Cancer Genetics Program, Beth Israel Deaconess Cancer Center, Departments of Medicine and Pathology, Beth Israel Deaconess Medical Center, Harvard Medical School, Boston, MA 02215.

Correspondence: Keiichi I. Nakayama, Department of Molecular and Cellular Biology, Medical Institute of Bioregulation, Kyushu University, 3-1-1 Maidashi, Higashi-ku, Fukuoka, Fukuoka 812-8582, Japan; e-mail: nakayak1@bioreg.kyushu-u.ac.jp.

References

1. Hosoya T, Maillard I, Engel JD. From the cradle to the grave: activities of GATA-3 throughout T-cell development and differentiation. *Immunol Rev.* 2010;238(1):110-125.
2. Naito T, Tanaka H, Naoe Y, Taniuchi I. Transcriptional control of T-cell development. *Int Immunol.* 2011;23(11):661-668.
3. Jameson SC, Bevan MJ. T-cell selection. *Curr Opin Immunol.* 1998;10(2):214-219.
4. Haks MC, Krimpenfort P, van den Brakel JH, Kruisbeek AM. Pre-TCR signaling and inactivation of p53 induces crucial cell survival pathways in pre-T cells. *Immunity.* 1999;11(1):91-101.
5. Jiang D, Lenardo MJ, Zúñiga-Pflücker JC. p53 prevents maturation to the CD4+CD8+ stage of thymocyte differentiation in the absence of T cell receptor rearrangement. *J Exp Med.* 1996;183(4):1923-1928.
6. Guidos CJ, Williams CJ, Grandal I, Knowles G, Huang MT, Danska JS. V(D)J recombination activates a p53-dependent DNA damage checkpoint in scid lymphocyte precursors. *Genes Dev.* 1996;10(16):2038-2054.
7. Sherr CJ, Roberts JM. Living with or without cyclins and cyclin-dependent kinases. *Genes Dev.* 2004;18(22):2699-2711.
8. Burkhart DL, Sage J. Cellular mechanisms of tumour suppression by the retinoblastoma gene. *Nat Rev Cancer.* 2008;8(9):671-682.
9. Polager S, Ginsberg D. p53 and E2f: partners in life and death. *Nat Rev Cancer.* 2009;9(10):738-748.
10. DeGregori J, Leone G, Miron A, Jakoi L, Nevins JR. Distinct roles for E2F proteins in cell growth control and apoptosis. *Proc Natl Acad Sci USA.* 1997;94(14):7245-7250.
11. Kowalik TF, DeGregori J, Schwarz JK, Nevins JR. E2F1 overexpression in quiescent fibroblasts leads to induction of cellular DNA synthesis and apoptosis. *J Virol.* 1995;69(4):2491-2500.
12. Phillips AC, Bates S, Ryan KM, Helin K, Vousden KH. Induction of DNA synthesis and apoptosis are separable functions of E2F-1. *Genes Dev.* 1997;11(14):1853-1863.
13. Qin XQ, Livingston DM, Kaelin WG Jr, Adams PD. Deregulated transcription factor E2F-1 expression leads to S-phase entry and p53-mediated apoptosis. *Proc Natl Acad Sci USA.* 1994;91(23):10918-10922.
14. Sherr CJ, Roberts JM. CDK inhibitors: positive and negative regulators of G1-phase progression. *Genes Dev.* 1999;13(12):1501-1512.
15. Deng C, Zhang P, Harper JW, Elledge SJ, Leder P. Mice lacking p21$^{CIP1/WAF1}$ undergo normal development, but are defective in G1 checkpoint control. *Cell.* 1995;82(4):675-684.
16. Nakayama K, Ishida N, Shirane M, et al. Mice lacking p27(^{Kip1}) display increased body size, multiple organ hyperplasia, retinal dysplasia, and pituitary tumors. *Cell.* 1996;85(5):707-720.
17. Fero ML, Rivkin M, Tasch M, et al. A syndrome of multiorgan hyperplasia with features of gigantism, tumorigenesis, and female sterility in p27(^{Kip1})-deficient mice. *Cell.* 1996;85(5):733-744.
18. Kiyokawa H, Kineman RD, Manova-Todorova KO, et al. Enhanced growth of mice lacking the cyclin-dependent kinase inhibitor function of p27(^{Kip1}). *Cell.* 1996;85(5):721-732.
19. Takahashi K, Nakayama K, Nakayama KI. Mice lacking a CDK inhibitor, p57^{Kip2}, exhibit skeletal abnormalities and growth retardation. *J Biochem.* 2000;127(1):73-83.
20. Zhang P, Liégeois NJ, Wong C, et al. Altered cell differentiation and proliferation in mice lacking p57^{KIP2} indicates a role in Beckwith-Wiedemann syndrome. *Nature.* 1997;387(6629):151-158.
21. Matsumoto A, Takeishi S, Kanie T, et al. p57 is required for quiescence and maintenance of adult hematopoietic stem cells. *Cell Stem Cell.* 2011;9(3):262-271.
22. Wolfer A, Bakker T, Wilson A, et al. Inactivation of Notch 1 in immature thymocytes does not perturb CD4 or CD8T cell development. *Nat Immunol.* 2001;2(3):235-241.
23. Wolfer A, Wilson A, Nemir M, MacDonald HR, Radtke F. Inactivation of Notch1 impairs VDJbeta rearrangement and allows pre-TCR-independent survival of early alpha beta Lineage Thymocytes. *Immunity.* 2002;16(6):869-879.
24. Matsuoka S, Edwards MC, Bai C, et al. p57^{KIP2}, a structurally distinct member of the p21^{CIP1} Cdk inhibitor family, is a candidate tumor suppressor gene. *Genes Dev.* 1995;9(6):650-662.
25. Laurent J, Bosco N, Marche PN, Ceredig R. New insights into the proliferation and differentiation of early mouse thymocytes. *Int Immunol.* 2004;16(8):1069-1080.
26. Cao Q, Xia Y, Azadniv M, Crispe IN. The E2F-1 transcription factor promotes caspase-8 and bid expression, and enhances Fas signaling in T cells. *J Immunol.* 2004;173(2):1111-1117.
27. Pant V, Quintás-Cardama A, Lozano G. The p53 pathway in hematopoiesis: lessons from mouse models, implications for humans. *Blood.* 2012;120(26):5118-5127.
28. DeGregori J. The genetics of the E2F family of transcription factors: shared functions and unique roles. *Biochim Biophys Acta.* 2002;1602(2):131-150.
29. Berkovich E, Ginsberg D. ATM is a target for positive regulation by E2F-1. *Oncogene.* 2003;22(2):161-167.
30. Fogal V, Kartasheva NN, Trigiante G, et al. ASPP1 and ASPP2 are new transcriptional targets of E2F. *Cell Death Differ.* 2005;12(4):369-376.